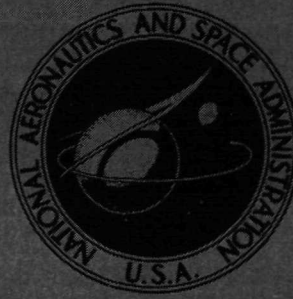


N73-11797

NASA TECHNICAL
MEMORANDUM



NASA TM X-2669

NASA TM X-2669

CASE FILE
COPY

METHODS FOR REDUCING BLADE PASSING
FREQUENCY NOISE GENERATED BY
ROTOR-WAKE - STATOR INTERACTION

by James H. Dittmar
Lewis Research Center
Cleveland, Ohio 44135

NATIONAL AERONAUTICS AND SPACE ADMINISTRATION • WASHINGTON, D. C. • NOVEMBER 1972

1. Report No. NASA TM X-2669	2. Government Accession No.	3. Recipient's Catalog No.	
4. Title and Subtitle METHODS FOR REDUCING BLADE PASSING FREQUENCY NOISE GENERATED BY ROTOR-WAKE - STATOR INTERACTION		5. Report Date November 1972	
		6. Performing Organization Code	
7. Author(s) James H. Dittmar		8. Performing Organization Report No. E-7066	
		10. Work Unit No. 501-04	
9. Performing Organization Name and Address Lewis Research Center National Aeronautics and Space Administration Cleveland, Ohio 44135		11. Contract or Grant No.	
		13. Type of Report and Period Covered Technical Memorandum	
12. Sponsoring Agency Name and Address National Aeronautics and Space Administration Washington, D.C. 20546		14. Sponsoring Agency Code	
		15. Supplementary Notes	
16. Abstract <p>A theoretical model for the generation of blade-passage noise caused by the interaction of rotor wakes with the downstream stator blades in a fan stage has been compiled. This model has combined a description of the rotor wake based on existing experimental correlations with an existing theory for the response of the stator blades to those wakes. This model of the interaction-caused blade-passage noise has been used to examine some effects of blade geometry and flow conditions on the noise generated. A set of significant parameters has been identified to reduce this interaction-caused blade-passage frequency noise. A redesign of an existing fan with the use of these concepts has produced a theoretical noise reduction of more than 7 decibels.</p>			
17. Key Words (Suggested by Author(s)) Sound; Noise; Aircraft; Fan; Jet; Wake; Lift; Rotor; Stator; Drag		18. Distribution Statement Unclassified - unlimited	
19. Security Classif. (of this report) Unclassified	20. Security Classif. (of this page) Unclassified	21. No. of Pages 31	22. Price* \$3.00

*For sale by the National Technical Information Service, Springfield, Virginia 22151

METHODS FOR REDUCING BLADE PASSING FREQUENCY NOISE GENERATED BY ROTOR-WAKE - STATOR INTERACTION

by James H. Dittmar

Lewis Research Center

SUMMARY

A theoretical model for the generation of blade-passage noise caused by the interaction of rotor wakes with the downstream stator blades in a fan stage was compiled. This model combined a description of the rotor wake based on existing experimental correlations with an existing theory for the response of the stator blades to those wakes. This model of the interaction-caused blade-passage noise was used to examine some effects of blade geometry and flow conditions on the noise generated.

With the use of the theoretical model, a set of significant aerodynamic parameters was identified to reduce this noise. The parameters were divided into two groups: (1) those that would reduce the rotor-blade wakes, and (2) those that would reduce the response of the stator blades to those wakes. Increasing the spacing between rotor and stator and reducing the rotor drag coefficient were indicated by the model as means of reducing the velocity defect in the rotor wakes that strike the stator blades. The stator blades respond to incoming velocity defects both parallel and perpendicular to their chords. The magnitude of both of those responses was reduced in theory by increasing ω , the reduced frequency parameter. This reduced frequency parameter, ω , was shown to increase with increasing stator chord and with increasing numbers of rotor blades. It was also indicated by the model that the parallel and perpendicular responses acted in opposite directions and could be used to partially cancel each other. This theoretical cancelling was accomplished by properly adjusting the velocity diagram of the flow behind the rotor and by adjusting the angle of attack of the stator blades.

An existing fan stage was examined with this model to determine where the fan stage could be improved. A redesign of this fan stage was done with the use of these noise-reducing concepts but without varying the rotor-stator spacing. This redesign resulted in a theoretical noise reduction of more than 7 decibels.

INTRODUCTION

Often, the most annoying noise generated by a fanjet engine is that occurring at the blade passing frequency of the fan. This sound not only occurs at a high sound pressure level but also usually occurs in the most sensitive frequency region of human hearing. In this report, a model for the generation of blade passing frequency noise is explored to determine the possibilities of reducing this noise at the source by design of the fan blade geometry and flow conditions of the fan stage.

For a complete fan stage, composed of rotor and stator blade rows, the generation of blade-passing discrete noise is often dominated by the interaction of rotor-blade wakes with the stator blades rather than by the rotor-alone noise (ref. 1). In addition to depending on the strength of the rotor wakes, the noise depends on the dynamic response of the stator blades to these wakes. This interaction-caused noise is generally considered to depend on the fluctuating lift of the stator blades.

Several investigators have modeled the fluctuating lift or dynamic response of an airfoil. One of the first of these models is that developed by Sears (ref. 2) and Kemp and Sears (ref. 3) for a flat plate in a transverse gust. This model has been extended by Horlock to include the response to a parallel gust (ref. 4). Other model variations or extensions appear in references 5 through 7. The Kemp and Sears model or one of its extensions has been used as the basis for several blade passing frequency prediction schemes of varying complexity (refs. 8, 9, and 10).

For the present report, the response model as given in reference 4, combined with a wake model, has been used to examine some effects of blade geometry and flow conditions on the fluctuating lift. This report concentrates on the noise-generation mechanism and does not include the effects of inlet and discharge ducts on the generated noise. In particular, this analysis does not include the duct cutoff frequency phenomena as related to optimum vane/blade ratio. The purpose of this investigation is to try to establish the significant variations of fan design parameters that will reduce the generated blade passing frequency noise and still be in the range of practicality.

The effects predicted by the model and the methods used are illustrated by reference to a previously tested fan stage (ref. 11). This fan stage is examined, by means of the model for the lift fluctuation, to determine how the noise of the fan stage might be reduced.

SYMBOLS

A_1 constant (see eq. (5))

A_2 constant (see eq. (6))

B	number of rotor blades
C	airfoil (rotor or stator) chord, length
C_D	profile drag coefficient
C_R	rotor chord, length
C_S	stator chord, length
$C_{X,1}$	axial velocity at rotor inlet, length/time (see fig. 4)
$C_{X,2}$	axial velocity at rotor exit, length/time (see fig. 4)
$C_{X,3}$	axial velocity at stator inlet, length/time (see fig. 4)
D	diffusion factor (see ref. 23)
i	$\sqrt{-1}$
$J_B(MB)$	Bessel function of order B and argument MB
l	incoming gust wavelength, length
ΔL_N	fluctuating lift, force/unit area
M	tip rotational Mach number
$S(\omega)$	transverse response function (see fig. 3)
$T(\omega)$	longitudinal response function (see fig. 3)
t	time
U	incoming velocity to airfoil, length/time
U_2	absolute velocity at rotor exit, length/time (see fig. 4)
U_3	absolute velocity at stator inlet, length/time (see fig. 4)
V	free-stream velocity at upstream blade-row inlet, length/time (see fig. 1)
V_1	relative velocity at rotor inlet, length/time (see fig. 4)
V_2	relative velocity at rotor exit, length/time (see fig. 4)
V_3	relative velocity at stator inlet, length/time (see fig. 4)
v_0	maximum difference from free stream velocity in the wake, length/time (see fig. 1)
W	rotor rotational velocity, length/time (see fig. 4)
X	distance from trailing edge of airfoil, length (see fig. 1)
α	angle of attack of stators relative to flow (angle between chord line and inlet flow direction), radians

β	relative flow angle at entrance to blade row, deg (see eq. (9))
β_1	relative flow angle at rotor inlet, deg (see fig. 4)
β_2	relative flow angle at rotor exit, deg (see fig. 4)
β_3	relative flow angle from rotor after translation to stator inlet, deg (see fig. 4)
$\bar{\beta}$	absolute flow angle at entrance to blade row, deg (see eq. (8))
$\bar{\beta}_2$	absolute flow angle at rotor exit, deg (see fig. 4)
$\bar{\beta}_3$	absolute flow angle at stator inlet, deg (see fig. 4)
β_∞	$\arctan [1/2 (\tan \beta_1 + \tan \beta_2)]$, deg
Γ	profile loss parameter (see ref. 23)
λ	stator setting angle (angle between chord line and axial direction), deg
ν	frequency of gust, radians/time
ρ	fluid density, mass/(length) ³
σ	rotor solidity (ratio of chord to circumferential spacing)
ψ	magnitude of gust variation, length/time
Ω	rotor wheel speed, revolutions/time
ω	reduced frequency ($\pi C/l$), radians/time
$\bar{\omega}_p$	profile loss coefficient (see ref. 23)

INTERACTION BETWEEN ROTOR AND STATOR

In many cases, the chief source of blade passing frequency noise is the interaction between rotor and stator. If the stator blade row is very close to the rotor, a potential interaction can exist. This potential interaction occurs when the flow field of the rotor is greatly affected by the presence of the stators. For recent quiet-fan designs, the blade rows are separated such that the potential interaction is no longer of significance. The viscous type interaction is then the prime source of blade passing frequency noise. This interaction occurs when the rotor blade wakes strike the stator blades and generate noise at the blade passing frequency. The general model used in this report for this blade passing frequency noise caused by viscous interaction is presented in the following section.

GENERAL MODEL

The rotor blades trail behind them a pattern of wakes that impinge on the stator blading. In the reference frame of an individual stator blade, the wake from every rotor blade is encountered every revolution. The frequency of the wake impingement is then the product of the number of rotor blades and the revolutions per unit time of the rotor (i. e., the blade passing frequency). The stator blades respond to the changes in incoming velocities and angles (the wakes) by generating a fluctuating lift force. This fluctuating force then represents the dipole noise source (ref. 12). The magnitude of the pressure fluctuation (noise) generated from this dipole source is directly proportional to the fluctuating force and occurs at the frequency of the fluctuating force. Any reduction in this fluctuating lift force then results directly in a reduction in noise. The model therefore includes a description of the rotor wakes and the response of the stators to the incoming wakes so as to determine the noise produced by the fluctuating lift.

Rotor Wakes

The wake behind an isolated airfoil has been investigated by a large number of researchers. It is the desire here to present some of these wake descriptions and to arrive at the formulation for the rotor wakes used in this report.

In 1938, Silverstein (ref. 13) indicated that, with the use of Prandtl's relations of reference 14, the maximum velocity defect in the wake of an airfoil (see fig. 1) should be of the following form:

$$\frac{v_o}{V} \approx \left(\frac{C_D}{\frac{X}{C_R}} \right)^{1/2} \quad (1)$$

This expression shows a square-root relation with both the drag coefficient and the inverse of the distance. In reference 13, the experimental data were fit by the expression

$$\frac{v_o}{V} = \frac{0.17}{\left(\frac{X}{C_R} + 0.05 \right)^{1/2}} \quad (2)$$

This expression has the square-root dependence with distance but does not show the variation with C_D . It was noted in reference 13 that the three airfoils tested had similar drag coefficients, ranging only from 0.0060 to 0.0073, and that perhaps for this reason the variation with C_D was not observed.

In 1939, Silverstein et al. (ref. 15) verified "... the predicted proportionality with $\sqrt{C_D}$." However, because of high values of v_o/V close to the trailing edge of the airfoil, the curve fit in reference 15 appeared to follow an inverse relation with distance instead of the inverse square root as expected. Silverstein states "... the inverse first power will be retained although it is recognized that an obvious inconsistency exists for large values of (X/C_R) ." This resulted in Silverstein using

$$\frac{v_o}{V} = \frac{2.42\sqrt{C_D}}{\left(\frac{X}{C_R} + 0.3\right)} \quad (3)$$

a relation used by many investigators in the noise field.

It should be noted that beyond the point $X/C_R = 0.5$, a curve varying with the inverse square root of distance fits Silverstein's data of reference 15 very well. This is shown in figure 2, a plot of data from reference 15, where the variation of equation (2) is plotted for $X/C_R = 0.5$ and greater. This good data fit indicates that the velocity defect should vary with the inverse square root of the distance behind the airfoil when the value of X/C_R is 0.5 or greater. Since the majority of the fan stages used in current turbofan engine designs have X/C_R greater than 0.5, the expression for the wake defect should vary with the inverse square root of the distance behind the airfoil. There are other, more recent, data which also indicate the variation with the square root of distance.

In 1953, Spence (ref. 16) investigated the growth of a turbulent wake behind an airfoil and found that a good fit to his data was

$$\frac{v_o}{V} = \frac{0.1265}{\left(\frac{X}{C_R} + 0.025\right)^{1/2}} \quad (4)$$

In 1956, Lieblein and Roudebush (ref. 17) fit the data from a number of airfoils and a number of cascades with a wake expression of the form

$$\frac{v_o}{V} = \frac{A_1}{\left(\frac{X}{C_R} + 0.025\right)^{1/2}} \quad (5)$$

It was found that the data fell between the curve for $A_1 = 0.075$ and the curve for $A_1 = 0.130$. The larger value of 0.130 corresponds to Spence's expression.

The range of the value of A_1 could possibly be because the expression should contain some function of the drag coefficient. If, as suggested by the work of Silverstein, the variation is with the square root of the drag coefficient, $\sqrt{C_D}$, then this variation in A_1 could be the result of a factor-of-three variation in the drag coefficient. It is likely that the data plotted in reference 17 had close to this factor-of-three variation in drag coefficient. From the previous considerations, it would then appear that the expression should contain the square root of the drag coefficient.

The previously stated references, particularly reference 17, which contains cascade data, demonstrate that the wake defect for a rotor wake varies with the square root of the distance behind the airfoil for X/C_R greater than 0.5. This is, then, the variation used in the present report.

References 14 and 15 also indicate that the wake defect varies with the square root of the drag coefficient. Since reference 15 showed the dependence on the square root of drag coefficient, and since it is likely that reference 17 contains it also, this square root of C_D is used in the wake model presented here.

The wake model used here is, then, of the form

$$\frac{v_o}{V} = \frac{A_2 \sqrt{C_D}}{\left(\frac{X}{C_R} + 0.025\right)^{1/2}} \quad (6)$$

Since the data of reference 13 are included in the plots of reference 17, it is possible to determine an approximate value for A_2 . From reference 13, $C_D \approx 0.0065$, and from reference 17, the recommended value of A_1 is 0.13. Therefore, $A_2 \sqrt{0.0065} = 0.13$. Then,

$$\frac{v_o}{V} = \frac{1.6 \sqrt{C_D}}{\left(\frac{X}{C_R} + 0.025\right)^{1/2}} \quad (7)$$

This approximation for the maximum velocity defect in the rotor wake is then used in the calculation of the fluctuating lift. It is recognized that the value of the drag coefficient depends on the operating condition of the blades. The manner in which the drag coefficient is evaluated, starting with the diffusion factor, is discussed later in this report.

Stator Response

Sears (ref. 2) determined the response of an isolated flat plate to a sinusoidal gust input transverse to the chord. In a fan stage, however, the stator experiences gusts in both the longitudinal and transverse directions. Horlock (ref. 4) added the response in the longitudinal direction and obtained the following expression for the response of a moving blade row to upstream wakes.

$$\Delta L_N = 2\pi\rho U \sin \bar{\beta} \psi e^{i\nu t} [S(\omega) - \alpha T(\omega) \cot \bar{\beta}] \quad (8)$$

where

ΔL_N	fluctuating lift, force/area
ρ	fluid density, mass/(length) ³
U	incoming velocity to airfoil, length/time
$\bar{\beta}$	absolute flow angle at entrance to blade row, deg
ψ	magnitude of gust variation, length/time
i	$\sqrt{-1}$
ν	frequency of gust, radians/time
t	time
$S(\omega)$	transverse response function (see fig. 3)
ω	reduced frequency ($\pi C_R/l$), radians/time
C	rotor chord, length
l	incoming gust wavelength, length
α	angle of attack of stators relative to flow (angle between chord line and inlet flow direction), radians
$T(\omega)$	longitudinal response function (see fig. 3)

To convert equation (8) for use on a stator blade downstream of the rotor, an additional angle β is needed to account for the different velocity diagram at the stator-inlet station, and the equation becomes

$$\Delta L_N = 2\pi\rho U \sin(\bar{\beta} + \beta)\psi e^{i\nu t} [S(\omega) - \alpha T(\omega) \cot(\bar{\beta} + \beta)] \quad (9)$$

where

β relative flow angle at entrance to blade row, deg

ω reduced frequency ($\pi C_S/l$), radians/time

C_S stator chord, length

To express this for a typical fan stage, the mean velocity diagrams are shown in figure 4. The axial velocity entering the rotor is $C_{X,1}$ and the relative velocity is V_1 . Using this relative velocity V_1 in the wake-defect equation (eq. (7)) yields

$$\frac{v_0}{V_1} = \frac{1.6 \sqrt{C_D}}{\left(\frac{X}{C_R} + 0.025\right)^{1/2}} \quad (10)$$

Exiting the rotor is the relative velocity V_2 , and with the addition of the rotor rotational velocity vector W , the absolute velocity is U_2 . The axial velocity $C_{X,2}$ is generally not equal to $C_{X,1}$, because of changes in the channel area across the rotor. At this rotor-exit station, the relative and absolute flow angles are β_2 and $\bar{\beta}_2$, respectively.

As the air moves further downstream, the changes in flow passage and flow conditions change the velocity diagram. At the entrance to the stator, the mean velocity relative to the rotor is V_3 , and the mean absolute velocity is U_3 . The relative flow angle is β_3 , and the absolute flow angle is $\bar{\beta}_3$.

When the velocities and flow angles shown in figure 4 are inserted into the stator response equation, the equation becomes

$$\Delta L_N = 2\pi\rho U_3 \sin(\bar{\beta}_3 + \beta_3)\psi e^{i\nu t} [S(\omega) - \alpha T(\omega) \cot(\bar{\beta}_3 + \beta_3)] \quad (11)$$

At the stator inlet, the flow varies with time. When a stator blade is immersed in a rotor wake, the absolute velocity (diagram C, fig. 5) entering the stator is less than the mean absolute velocity U_3 . When the stator is in the maximum flow between blades (diagram A, fig. 5), the velocity is greater than the mean velocity U_3 . On the relative-

velocity side of these velocity diagrams, the difference between the maximum flow velocity between the blades (diagram A) and the wake minimum velocity (diagram C) is the amount of the maximum velocity defect in the wake v_0 . The magnitude of the sinusoidal fluctuation about the mean is then one-half the maximum velocity defect in the wake, or $v_0/2$.

With $\psi = v_0/2$, the combination of the rotor wake model (eq. (10)), and the stator response (eq. (11)) gives the following expression for the fluctuating lift generated by the viscous interaction:

$$\Delta L_N = \pi \rho U_3 V_1 \sin(\bar{\beta}_3 + \beta_3) \left[\frac{1.6 \sqrt{C_D}}{\left(\frac{X}{C_R} + 0.025\right)^{1/2}} \right] e^{i\omega t} [(S(\omega) - \alpha T(\omega) \cot(\bar{\beta}_3 + \beta_3)] \quad (12)$$

Because the dipole noise, in sound pressure level (SPL), varies as the square of the pressure $[\text{SPL} = 10 \log_{10} (P/P_{\text{ref}})^2 = 20 \log_{10} (P/P_{\text{ref}})]$ and the pressure varies directly with ΔL_N , a decibel change in $(\Delta L_N)^2$ results in a decibel change in SPL.

This is, then, the model that will be used to develop a systematic procedure for reducing this interaction-caused blade passing frequency noise. Benzakein and Kazin (ref. 8) have developed a similar model for the fluctuating lift on a blade row. Their model, however, includes a wake defect model that decays with the inverse of spacing (eq. (3)) instead of the inverse square root (eq. (7)) as used in this report. In addition, the model in reference 8 only includes the transverse gust response and does not also include the longitudinal gust response, as included herein.

It should be noted that the response of the stator blades (eq. (11)) is based on isolated flat plate theory. The effects of typical blade cambers and solidities in a cascade are expected to change somewhat the values of fluctuating lift and thus noise. At the present time, it is not known exactly what these effects will be. Stator response by equation (3) is used here because of the ease of application and because it seems to provide a reasonable approximation to what happens in the actual situation.

SIGNIFICANT TERMS IN NOISE REDUCTION

The purpose of this section is to show how the proper choice of aerodynamic parameters can result in less fluctuating lift and thus less noise. The expression for the fluctuating part of the stator lift (eq. (12)) indicates a number of terms that are significant in reducing the blade passing frequency noise. The first terms encountered are those involving the velocities U_3 and V_1 . The reduction of these velocities would

result in a decreased lift fluctuation. These velocities are, in general, functions of the desired overall pressure ratio, wheel speed, mass flow, and bypass ratio of the stage. Since the desired overall pressure ratio, mass flow, and bypass ratio would probably be fixed for a particular design, lower wheel speeds seem to be the means of lowering the velocities. However, as the wheel speed is lowered, the amount of loading on the blade increases to achieve the same pressure ratio, thereby possibly increasing the noise. Therefore, it may be necessary to compromise between the lowest possible wheel speed and some other desired noise-reducing parameters. This will be discussed somewhat in later sections. Because of the desire to avoid multiple pure tones, caused by shock waves on the blade leading edges, the rotor-tip rotational speed will be maintained subsonic for this work.

The following is an evaluation of the remainder of the significant terms in the expression (eq. (12)) for the fluctuating lift. The terms are presented roughly in their order of occurrence in the equation and not necessarily in their order of importance.

Rotor Wakes

Spacing between rotor and stator. - The amount of spacing between rotor and stator has been shown to have an effect on the noise generated. Lowson (ref. 18) has indicated from available data that the noise decays at the rate of approximately 2 decibels per doubling of the spacing between rotor and stator when X/C_R is greater than 1.0. Figure 6 shows the decibel decay of the wake model presented herein (eq. (10)) and Silverstein's model from reference 15 (eq. (3)), along with the 2 decibels per doubling indicated by Lowson. The curve generated by Lowson is based on a number of different authors' experiments and appears to be typical of the noise variation with spacing. Lowson's curve is more nearly approximated by equation (10), the model used in this report, than by equation (3). Equation (10) appears to be the preferred model for the wake decay, particularly when it is recognized that some scatter existed in the data presented by Lowson.

The wake model used in this report indicates approximately 3 decibels of noise reduction for a doubling of the spacing between rotor and stator. This indicates, as is shown by experiment, that an increase in spacing between rotor and stator is a relatively important method for reducing interaction-caused blade passing frequency noise.

Profile drag coefficient. - As can be seen from the wake model (eq. (10)), the profile drag coefficient C_D has an effect on the maximum rotor wake velocity defect. The wake defect increases with increasing C_D . Figure 7 shows the effect of C_D on the noise generated and indicates the desirability of reducing the rotor drag coefficient.

Shepherd (ref. 19, p. 402; fig. 10.8) has indicated that, in the normal design range

($+5^\circ$ to -5° incidence), as the rotor turning increases, the drag coefficient increases. Besides having larger values of the profile drag coefficient, the blades with higher turning generally exhibit a decrease in the range over which their minimum C_D is observed. An example of this is shown in reference 20 (p. 193, fig. 86), where the operating range decreases for increasing turning. This decrease in operating range means the rotor blades are more susceptible to disturbances upstream of the rotor, which results in larger rotor wakes. Thus, for both noise and aerodynamic benefits, it is desirable to keep rotor turning at a low value.

Since the pressure ratio is a function of the wheel speed and the rotor turning, the desire to lower the rotor turning would be in opposition to the lowering of the wheel speed of a fan while maintaining the overall pressure ratio. A complicated compromise is indicated here, for if the wheel speed is too high, the fluctuating lift increases because of the increase in the velocity terms (U_3, V_1). If the wheel speed is too low, the turning increases, thereby increasing the fluctuating lift through increasing drag coefficient. An optimum wheel speed would then exist for each stage, and a number of calculations might be needed before this optimum is obtained.

As the hub section of a fan rotor requires more turning for a given pressure ratio than a tip section, it may be necessary to trail off the pressure ratio toward the hub, being careful not to go below the value needed for a reasonable core engine flow. This would lower the amount of turning at the hub, and the overall pressure ratio could be maintained by boosting the desired pressure ratio at the other sections.

Stator Response

Reduced frequency. - The response of the stators to the rotor wakes appears to be an area where a significant contribution can be made to the noise reduction. Figure 3 shows that as the reduced frequency ω is increased, the individual response functions $S(\omega)$ and $T(\omega)$ become lower in magnitude. (The magnitude of the response function in the complex plane is the length of a vector drawn from the origin to the response curve at the value of ω under consideration.) A plot of $|S(\omega)|$ against ω is shown in figure 8. Figure 9 shows a plot of SPL reduction against ω for $|S(\omega)|$ and $|T(\omega)|$.

The reduced frequency ω is equal to $\pi C_S/l$, where C_S is the stator chord, and l is the incoming gust wavelength. Increasing the stator chord, while maintaining a constant solidity, would increase ω and would then bring about a reduction in fluctuating lift. This can be seen by imagining two airfoils, one long and one short with respect to the wavelength of an incoming velocity gust. The short airfoil would experience the total variation of an incoming velocity gust. The longer airfoil would experience a number of gust wavelengths over its chordal length, each one partially cancelling out

some of the effects of the others, and would, therefore, experience less variation in total lift than the short airfoil.

The incoming-gust wavelength could be represented by the velocity of the incoming gusts divided by a product of the rotor blade number and the speed of the rotor:

$$\lambda = \frac{C_{X,3}}{B\Omega} \quad (13)$$

As a decrease in λ brings about an increase in ω and, therefore, a noise reduction, this points to larger rotor blade numbers as a means of reducing interaction noise.

The increase in rotor blade number also decreases the noise generated by the rotor alone. In the propeller-alone noise theory presented by Gutin (ref. 21) and Morse and Ingard (ref. 22), the dominant term is of the form $J_B(MB)$. For the same rotational Mach number M , this term decreases significantly as B increases. For example, with M equal to 0.89, $J_B(MB)$ is 0.0211 when B is 40, but $J_B(MB)$ decreases to 0.0084 when the number of blades is 60. The increase in rotor-blade number, then, appears to be a doubly profitable change, for it reduces the blade passing frequency noise caused both by interaction and by the rotor-alone mechanisms.

Cancellation of lift fluctuating components. - The difference in signs between the terms containing the two response functions $S(\omega)$ and $T(\omega)$ in equation (12) indicates the possibility of large reductions in interaction-caused noise. Since the fluctuations in the lift caused by longitudinal and transverse gusts act in opposite ways, they may be used to cancel each other. Another way to examine the stator lift response is by means of figure 5. In this example, the velocity diagram B represents the mean velocity of the flow. Diagram C represents the flow when the stator is passing through a wake. As the rotor wake strikes the stator blade, the velocity of the flow on the stator decreases (diagram C). This represents a lowering of the stator lift. At the same time, however, the angle of attack of the air on the stators is increasing. This represents an increase in stator lift. As the blade moves out of the rotor wakes, the opposite occurs (i.e., the velocity increases, thereby increasing lift, while the angle of attack decreases, thereby decreasing lift). In both cases, the two terms containing $S(\omega)$ and $T(\omega)$ have a cancelling effect.

To take advantage of this cancelling effect, the term $\alpha \cot(\overline{\beta}_3 + \beta_3)$ (see eq. (12)) must be adjusted to more completely cancel the two response functions. Table I, taken from reference 4, shows the relative magnitudes of $S(\omega)$ and $T(\omega)$ at various values of the reduced frequency.

The sum of the angles $\overline{\beta}_3$ and β_3 is fairly well set by the design specifications for the rotor and the flow passage contours. Therefore, changes in $\overline{\beta}_3$ and β_3 would involve a complicated series of iterations between the sum of the angles and the design parameters. A change in $(\overline{\beta}_3 + \beta_3)$ can result in a significant noise reduction and

should not be eliminated completely from consideration. The example fan redesign presented in the next section of this report does show how this variation at the hub section reduces the noise. It is easier to change the angle of attack α of the stator than to change $\overline{\beta}_3$ and β_3 . Therefore, changing α seems to be the better way to accomplish the desired cancellation. It should be noted that because each spanwise section of the blade would have different conditions, this cancellation would have to be worked out at varying radial locations from hub to tip.

According to the present theory, this method could provide for almost complete cancellation of the fluctuating lift. Because of possible stall conditions of the stator blades, a limit is placed on the range over which the angle of incidence to the stator blades can be varied. These aerodynamic limitations still leave the ability to provide a significant portion of the cancellation. Therefore, a reduction in noise could be made by matching as well as possible the value of $\alpha \cot(\overline{\beta}_3 + \beta_3)$ that would provide cancellation of the response terms.

EXAMPLE OF NOISE-REDUCTION METHOD

In order to illustrate the application of this method, an existing fan design is chosen as a base. A new design is then formulated to reduce the interaction-caused blade passing frequency noise.

Since each spanwise section of the blade is acting differently, 11 sections (tip to hub) are chosen for this analysis. The magnitude of the lift fluctuation is computed from the following expression:

$$|\Delta L_N| = \left| \pi \rho \frac{1.6 \sqrt{C_D}}{\left(\frac{X}{C_R} + 0.025\right)^{1/2}} U_3 V_1 \sin(\overline{\beta}_3 + \beta_3) [S(\omega) - \alpha \cot(\overline{\beta}_3 + \beta_3) T(\omega)] \right|$$

Since $S(\omega)$ and $T(\omega)$ are approximately in phase in the real, imaginary plane for $\omega > 1$, they are replaced with $|S(\omega)|$ and $|T(\omega)|$ (see fig. 3):

$$|\Delta L_N| = \left| \pi \rho \frac{1.6 \sqrt{C_D}}{\left(\frac{X}{C_R} + 0.025\right)^{1/2}} U_3 V_1 \sin(\overline{\beta}_3 + \beta_3) [|S(\omega)| - \alpha \cot(\overline{\beta}_3 + \beta_3) |T(\omega)|] \right|$$

As most blade design programs do not give a computed value of C_D , it is necessary to determine one for use in the proposed calculation. The design program that was used

in designing these fans computes a diffusion factor D (see ref. 23) and with this determines a profile loss coefficient $\overline{\omega}_p$ from input curves of loss parameter Γ against diffusion factor (see ref. 23). The same curves of loss parameter against diffusion factor were used in both these designs.

Shepherd (ref. 19, p. 189) gives the following expression for C_D , which is used in the present analysis:

$$C_D = \frac{\overline{\omega}_p \cos^3 \beta_\infty}{\sigma \cos^2 \beta_1}$$

This expression is exact only when the inlet and exit axial velocities are equal, but it is considered to be a good approximation for most fan designs.

The stator angle of attack is computed by taking the difference of the flow angle and the blade setting angle λ :

$$\alpha = \overline{\beta}_3 - \lambda$$

The method described in this report was first applied to the base fan to determine where improvements could be made. Then, a new fan was designed to incorporate these noise-reduction factors.

Base Fan

The base fan stage had 53 rotor blades, 112 stator blades, and an overall pressure ratio of 1.5. The tip speed of the base fan was approximately 335 meters per second (1100 ft/sec). The rotor chord was 13.97 centimeters (5.5 in.), and the stator chord was 6.78 centimeters (2.67 in.). The rotor tip diameter was 1.83 meters (72 in.). The particular design numbers used in this analysis are shown in table II.

The axial spacing of this fan was about 4 rotor chords at the tip between rotor and stator. The reduced frequency, calculated with the axial velocity ($C_{X,3}$) of 213.4 meters per second (700 ft/sec), was approximately the same from hub to tip and equal to 3.1. With this value of the reduced frequency, the values of $|S(\omega)|$ and $|T(\omega)|$ were 0.24 and 0.72, respectively. When the analysis was applied to the base fan the following lift pressure fluctuations were obtained for each section:

Blade section	Lift-pressure fluctuation	
	N/m ²	lb/ft ²
1 (tip)	191.6	3.98
2	113.0	2.34
3	68.2	1.43
4	53.6	1.12
5	43.4	.907
6	40.7	.851
7	32.1	.669
8	16.2	.339
9	12.4	.260
10	77.0	1.61
11 (hub)	225.0	4.73
Total	873.2	18.24
Average	≈79.4	≈1.66

Since each section had approximately the same blade area, the lift fluctuations were added with each section rated equally, and an average value was taken.

Rotor wakes. - The section lift-fluctuation values show that the hub is a large noise contributor. This particular fan has a constant hub-to-tip pressure ratio at the rotor outlet of 1.541. This required pressure ratio at all spanwise stations results in large amounts of rotor turning ($\approx 60^\circ$, $\beta_1 - \beta_2$ in table II) at the hub.

The large amount of rotor turning gives rise to a larger maximum velocity defect in the rotor wake. This situation indicates that the required pressure ratio at the rotor hub should be decreased and the tip speed should be slightly increased so as to decrease the rotor turning at the hub.

Stator response. - As can be seen from figure 9, an increase in ω could result in measurable noise reduction. In order to increase the reduced frequency parameter ω , the number of rotor blades could be increased and the stator-blade chord could be lengthened.

As no attempt was made in the design of this base fan to provide for lift fluctuation cancellation, the fan might be improved by this method. The stator-blade angles of attack could be adjusted at each section to maximize the cancellation. In addition, a reduction in rotor turning near the hub would improve the flow angles into the stators. As the turning is lowered, the angles $\overline{\beta_3}$ and β_3 , through the term $\alpha \cot \overline{\beta_3} + \beta_3$ from equation (12), come closer to providing a cancellation between the response functions.

Improved Fan

A new fan, which attempted to improve the areas found deficient in the base fan, was then designed. Some of the restrictions on the new fan were that it have the same overall stage pressure ratio and mass flow rate as the base fan and that the spacing between rotor and stator be approximately the same (i. e., ≈ 4 rotor chords) because of length limitations. A description of the improvements in this fan are now presented.

The first step in reducing the noise of this fan was to reduce the rotor turning by trailing off the pressure ratio near the hub and by slightly increasing the tip speed. The tip speed was increased from approximately 335 meters per second (1100 ft/sec) to 347 meters per second (1140 ft/sec). The pressure ratio behind the rotor was slightly increased at the tip to 1.556 and trailed off at the hub to 1.375 (see table III). This gave the same overall fan pressure ratio of 1.5 as did the base fan.

In order to boost the reduced frequency parameter ω , the number of rotor blades was increased to 60, and the rotor chord was reduced to 12.7 centimeters (5 in.). This increase in the number of rotor blades also helped to reduce the rotor-alone noise and to counteract the noise increase of the slightly higher tip speed (see stator response section). The stator chord was approximately doubled to 12.3 centimeters (4.83 in.) in order to increase ω .

In this particular case, the increased stator chord with a reasonable solidity yielded 71 stator blades. This violates the optimum vane/blade ratio (ref. 24). Therefore, it may allow a larger portion of the generated noise to propagate out the fan ducting and possibly negate some of the noise benefit gained by increasing ω . As the base fan was theoretically "cut off" and still was dominated by blade passing frequency noise (ref. 11), this may not be too serious. It should be noted that, for this base fan, most of the noise reduction could still be obtained without this large an increase in ω if the optimum vane/blade ratio were to be maintained.

A calculation of the reduced frequency for this fan resulted in ω equal to 6.6. With this reduced frequency, the magnitudes of $S(\omega)$ and $T(\omega)$ were 0.17 and 0.53, respectively.

The angle of attack was varied on the stators to provide as much lift fluctuation cancellation as was reasonable while maintaining good stator aerodynamics. The incidence to the suction surface of the stator blades varied from 3 degrees at the tip to zero at the hub, as is shown in table IV. This, combined with the reduced rotor-turning improvement of the incoming hub flow, enhanced the cancellation of the lift-fluctuation components.

All of these considerations resulted in a fan as shown in table V. The hub section rotor turning was reduced to 40° , which represented a 20° reduction in the amount of

rotor turning. With this reduction in rotor turning, the pressure ratio was reduced to 1.375 at the hub (see table III).

These changes resulted in the following calculated values for lift-pressure fluctuation:

Blade section	Lift-pressure fluctuation	
	N/m ²	lb/ft ²
1 (tip)	133.2	2.79
2	70.3	1.47
3	43.6	.908
4	33.1	.689
5	26.0	.545
6	22.8	.473
7	19.6	.409
8	11.7	.246
9	.1	.003
10	2.79	.039
11 (hub)	9.59	.201
Total	372.8	7.77
Average	≈33.9	0.707

As can be seen, the new fan has reduced the lift fluctuation at all sections, with the largest reductions at the hub. For a calculation of the relative interaction-caused blade passage frequency noise of these two fans, the ratio of the averages is calculated and 20 times the logarithm to the base 10 is taken of this ratio:

$$\text{Decibels of noise} = 20 \log_{10} \left(\frac{\text{Average lift fluctuation of improved fan}}{\text{Average lift fluctuation of base fan}} \right)$$

(If the total blade area of the two stators were significantly different, an area-ratio factor would also be included.) This calculation gave a theoretical noise reduction of over 7 decibels.

The application of this method has resulted in a sizeable theoretical noise reduction for this particular fan. The application of this method to other fans would be expected to reduce their interaction-caused blade passing frequency noise. The amount of the noise reduction would depend on the particular fan being investigated, but it possibly could be greater than the 7 decibels calculated for this fan redesign.

SUMMARY OF RESULTS

A set of significant aerodynamic parameters have been identified to reduce blade passing frequency noise caused by viscous interaction. The parameters break into two groups: those that reduce the rotor blade wakes, and those that reduce the response of the stator blades to these wakes. This stator response is based on isolated flat-plate theory. The pertinent results are as follows:

To reduce and control the velocity defect in the rotor wakes striking the stator:

1. Increase the spacing between rotor and stator.
2. Reduce the rotor drag coefficient.

To reduce the response of the stator blades:

1. Increase the reduced frequency ω by
 - (a) increasing the stator chord
 - (b) increasing the number of rotor blades
2. Adjust $\alpha \cot(\overline{\beta_3} + \beta_3)$ to provide as much cancellation of the stator response function terms as possible, by
 - (a) varying the angle of attack α
 - (b) varying the angle $(\overline{\beta_3} + \beta_3)$ between the absolute and relative velocities behind the rotor through changes in the rotor (such as the amount of rotor turning, etc.)

By applying these ideas to an existing fan, a theoretical reduction of over 7 decibels was calculated. The application of this theory to other fans should predict a noticeable reduction in their blade passing frequency noise caused by viscous interaction.

Lewis Research Center,
National Aeronautics and Space Administration,
Cleveland, Ohio, August 30, 1972,
501-04.

REFERENCES

1. Sharland, I. J.: Sources of Noise in Axial Flow Fans. *J. Sound Vib.*, vol. 1, no. 3, 1964, pp. 302-322.
2. Sears, William R.: Some Aspects of Non-Stationary Airfoil Theory and Its Practical Application. *J. Aeron. Sci.*, vol. 8, no. 3, Jan. 1941, pp. 104-108.
3. Kemp, Nelson, H.; and Sears, W. R.: The Unsteady Forces Due to Viscous Wakes in Turbomachines. *J. Aeron. Sci.*, vol. 22, no. 7, July 1955, pp. 478-483.
4. Horlock, J. H.: Fluctuating Lift Forces on Aerofoils Moving Through Transverse and Chordwise Gusts. *J. Basic Eng.*, vol. 90, no. 4, Dec. 1968, pp. 494-500.
5. Arnoldi, Robert A.: Unsteady Airfoil Response. *Basic Aerodynamic Noise Research*. NASA SP-207, 1969, pp. 247-256.
6. Filotas, L. T.: Response of an Infinite Wing to an Oblique Sinusoidal Gust: A Generalization of Sears' Problem. *Basic Aerodynamic Noise Research*. NASA SP-207, 1969, pp. 231-246.
7. Henderson, R. E.: Theoretical Analysis of the Fluctuating Lift on the Rotor of an Axial Turbomachine. Rep. TM 505-03, Pennsylvania State Univ., Ordnance Research Lab., Dec. 1970 (Work done under Contract N00017-70-C-1407.)
8. Benzakein, M. J.; and Kazin, S. B.: Fan Compressor Noise Reduction. Paper 69-GT-9, ASME, Mar. 1969.
9. Mani, Ramani: Discrete Frequency Noise Generation From an Axial Flow Fan Blade Row. Paper 69-FE-12, ASME, June 1969.
10. Ollerhead, J. B.; and Munch, C. L.: An Application of Theory to Axial Compressor Noise. NASA CR-1519, 1970.
11. Goldstein, Arthur W.; Lucas, James G.; and Balombin, Joseph R.: Acoustic and Aerodynamic Performance of a 6-Foot-Diameter Fan for Turbofan Engines. 2: Performance of QF-1 Fan in Nacelle Without Acoustic Suppression. NASA TN D-6080, 1970.
12. Morse, Philip M.; and Ingard, K. Uno: *Theoretical Acoustics*. McGraw-Hill Book Co., Inc., 1968, p. 312.
13. Silverstein, Abe: Wake Characteristics and Determination of Profile Drag by the Momentum Method. *Proceedings of the Fifth International Congress for Applied Mechanics*, 1938, pp. 403-409.

14. Prandtl, L.: The Mechanics of Viscous Fluids. Spread of Turbulence. Vol. III, div. 6, sec. 25 of Aerodynamic Theory. W. F. Durand, ed., Julius Springer, Berlin, 1935, p. 165.
15. Silverstein, Abe; Katzoff, S.; and Bullivant, W. Kenneth: Downwash and Wake Behind Plain and Flapped Airfoils. NACA TR 651, 1939.
16. Spence, D. A.: Growth of the Turbulent Wake Close Behind an Aerofoil at Incidence. Rep. ARC-CP-125, Aeronautical Research Council, Gt. Britain, 1953.
17. Lieblein, Seymour; and Roudebush, William H.: Low-Speed Wake Characteristics of Two-Dimensional Cascade and Isolated Airfoil Sections. NACA TN 3771, 1956.
18. Lowson, M. V.: Reduction of Compressor Noise Radiation. J. Acoust. Soc. Am., vol. 43, no. 1, Jan. 1968, pp. 37-50.
19. Shepherd, D. G.: Principles of Turbomachinery. Macmillan Co., 1961.
20. Emery, James C.; Herrig, L. Joseph; Erwin, John R.; and Felix, A. Richard: Systematic Two-Dimensional Cascade Tests of NACA 65-Series Compressor Blades at Low-Speeds. NACA TR-1368, 1958.
21. Gutin, L.: On the Sound Field of a Rotating Propeller. NACA TM-1195, 1948.
22. Morse, Philip M.; and Ingard, K. Uno: Theoretical Acoustics. McGraw-Hill Book Co., Inc., 1968, pp. 738-748.
23. Johnsen, Irving A.; and Bullock, Robert O., eds.: Aerodynamic Design of Axial-Flow Compressors. NASA SP-36, 1965.
24. Tyler, J. M.; and Sofrin, T. G.: Axial Flow Compressor Noise Studies. Trans. SAE, vol. 70, 1962, pp. 309-332.

TABLE I. - VALUES OF TRANSVERSE AND LONGITUDINAL
RESPONSE FUNCTIONS

[From reference 4.]

Reduced frequency, ω	Transverse response function, $S(\omega)$	Magnitude of transverse response function, $ S(\omega) $	Longitudinal response function, $T(\omega)$	Magnitude of longitudinal response function, $ T(\omega) $
0	1.0	1.0	2.0	2.0
.1	0.821 - 0.164i	.837	1.819 - 0.114i	1.82
.2	0.702 - 0.160i	.720	1.692 - 0.060i	1.69
.3	0.624 - 0.126i	.637	1.602 + 0.022i	1.60
.4	0.568 - 0.085i	.574	1.528 + 0.111i	1.53
.5	0.525 - 0.044i	.527	1.463 + 0.198i	1.48
.7	0.456 + 0.032i	.457	1.337 + 0.361i	1.38
1.0	0.369 + 0.126i	.390	1.134 + 0.566i	1.27
2.0	0.082 + 0.268i	.280	0.306 + 0.845i	.899
2.5	-0.048 + 0.247i	.252	-0.096 + 0.744i	.750
3.5	-0.145 + 0.178i	.230	-0.525 + 0.315i	.612
5.0	-0.081 - 0.159i	.178	-0.259 - 0.487i	.522

TABLE II. - DESIGN PARAMETERS FOR BASE FAN

Blade section	Fluid density, ρ		Absolute velocity at stator inlet, U_3		Relative velocity at rotor inlet, V_1		Relative flow angle from rotor after translation to stator inlet, β_3' , deg	Absolute flow angle at stator inlet, β_3' , deg	Stator setting angle (angle between chord line and axial direction), λ , deg	Diffusion factor, D	Profile loss coefficient, $\frac{\omega_p}{\omega_p}$	Rotor solidity, σ	Relative flow angle at rotor inlet, β_1' , deg	Relative flow angle at rotor exit, β_2' , deg
	kg/m ³	lbm/ft ³	m/sec	ft/sec	m/sec	ft/sec								
1 (tip)	1.262	0.0788	251.2	824	374.9	1230	40.71	37.89	8.03	0.4595	0.1884	1.343	66.55	42.37
2	1.275	.0796	251.5	825	369.1	1211	41.39	34.31	7.53	.4403	.1063	1.372	62.53	42.35
3	1.277	.0797	253.9	833	362.4	1189	40.04	33.06	7.41	.4393	.0576	1.414	59.32	41.32
4	1.269	.0792	257.3	844	354.2	1162	38.09	33.31	7.74	.4589	.0472	1.466	56.70	38.99
5	1.256	.0784	260.3	854	345.0	1132	33.92	33.98	8.26	.4832	.0486	1.531	54.47	35.78
6	1.245	.0777	264.3	867	334.4	1097	31.79	35.31	8.87	.5053	.0527	1.611	52.45	31.44
7	1.229	.0767	269.1	883	332.5	1058	27.13	37.27	9.62	.5243	.0609	1.707	50.51	25.76
8	1.213	.0757	274.0	899	309.4	1015	21.01	39.49	10.56	.5277	.0751	1.827	48.57	18.33
9	1.197	.0747	279.2	916	295.4	969	13.17	42.23	11.84	.5391	.0976	1.982	46.50	8.56
10	1.181	.0737	285.9	938	279.8	918	1.26	46.54	13.68	.5149	.1323	2.1906	44.11	-4.1
11 (hub)	1.160	.0724	296.6	973	264.3	867	-16.86	53.06	16.55	.4601	.1929	2.4915	41.03	-19.9

TABLE III. - PRESSURE RATIO

AT ROTOR EXIT

Blade section	Pressure ratio		
	Base fan	Improved fan	
1 (tip)	1.541	1.556	
2	↓	↓	
3			
4			
5			
6			
7			
8			
9			1.545
10			1.427
11 (hub)			1.375

TABLE IV. - ANGLE OF INCIDENCE

TO SUCTION SURFACE OF

STATOR BLADE

Blade section	Angle of incidence, deg			
	Base fan	Improved fan		
1 (tip)	0	3.0		
2	↓	↓		
3				
4				
5				
6			2.5	
7			2.0	
8			1.5	
9			1.0	
10			0	
11 (hub)				

TABLE V. - DESIGN PARAMETERS FOR IMPROVED FAN

Blade section	Fluid density, ρ		Absolute velocity at stator inlet, U_3		Relative velocity at rotor inlet, V_1		Relative flow angle from rotor after translation to stator, inlet, β_3 , deg	Absolute flow angle at stator inlet, β_3 , deg	Stator setting angle (angle between chord line and axial direction), λ , deg	Diffusion factor, D	Profile loss coefficient, $\overline{\omega}_p$	Rotor solidity, σ	Relative flow angle at rotor inlet, β_1 , deg	Relative flow angle at rotor exit, β_2 , deg
	kg/m ³	lbm/ft ³	m/sec	ft/sec	m/sec	ft/sec								
1 (tip)	1.267	0.0791	252.4	828	385.6	1265	41.6	37.4	7.79	0.4540	0.1953	1.360	67.69	45.38
2	1.283	.0801	253.0	830	380.1	1247	40.5	33.8	7.08	.4282	.1072	1.416	63.41	45.10
3	1.285	.0802	254.8	836	373.4	1225	38.8	32.6	7.04	.4305	.0642	1.476	60.09	43.84
4	1.280	.0799	257.6	845	365.2	1198	36.3	32.8	7.65	.4481	.0522	1.542	57.46	41.51
5	1.274	.0795	260.3	854	355.4	1166	33.4	33.5	8.40	.4670	.0455	1.616	55.26	38.53
6	1.262	.0788	264.0	866	344.1	1129	29.9	34.8	9.40	.4902	.0514	1.702	53.30	34.38
7	1.248	.0779	267.9	879	331.3	1087	25.4	36.8	10.86	.5159	.0691	1.804	51.46	28.65
8	1.237	.0772	271.9	892	317.3	1041	20.1	39.2	12.50	.5338	.0858	1.928	49.61	21.33
9	1.229	.0767	272.2	893	301.4	989	14.2	42.1	14.42	.5387	.1031	2.085	47.64	12.73
10	1.214	.0758	249.6	819	284.1	932	14.6	42.4	15.01	.4981	.1354	2.293	45.34	10.96
11 (hub)	1.208	.0754	235.0	771	266.4	874	7.2	47.9	18.17	.4810	.1912	2.593	42.24	1.20

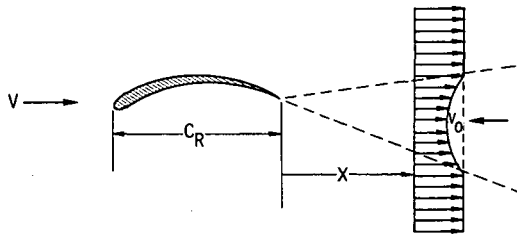


Figure 1. - Wake model.

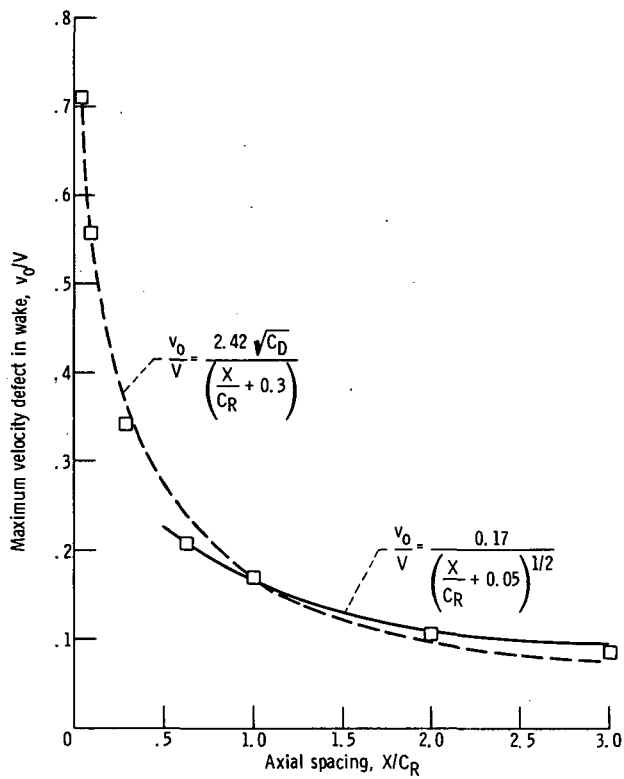


Figure 2. - Wake defect. (Data from ref. 15.)

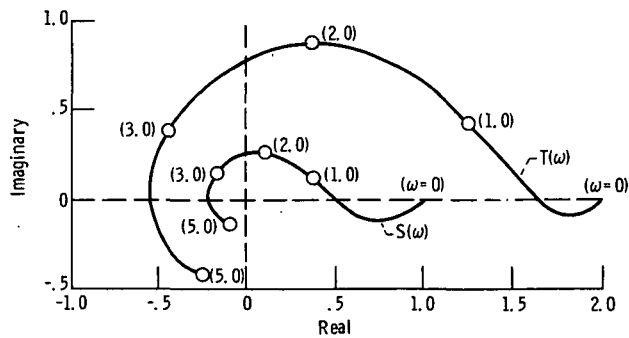


Figure 3. - Response functions $S(\omega)$ and $T(\omega)$. Numbers in parentheses are values of reduced frequency ω . (Data from ref. 4.)

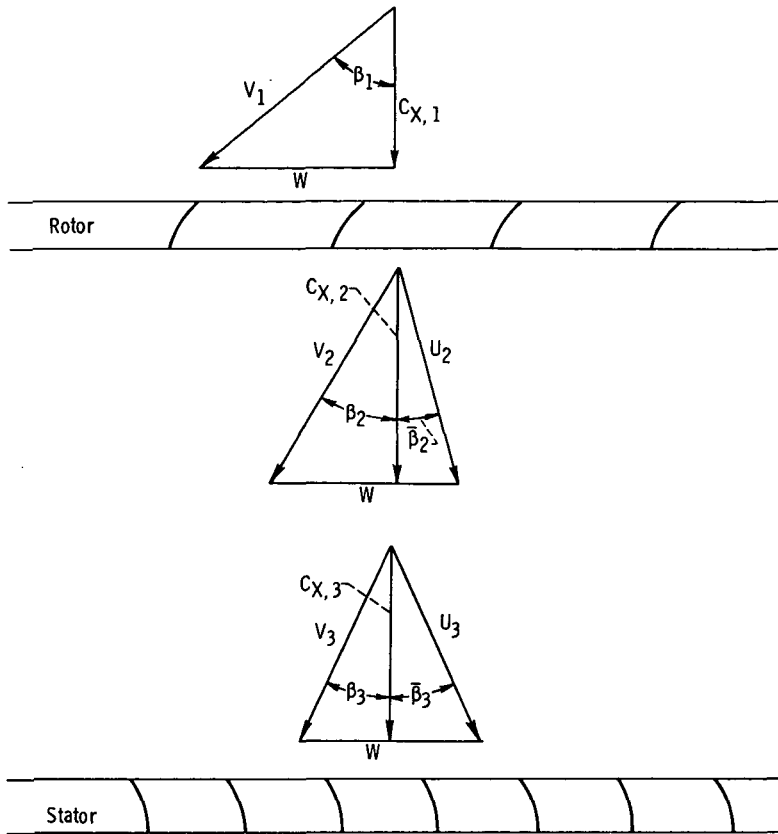


Figure 4. - Mean velocity diagrams.

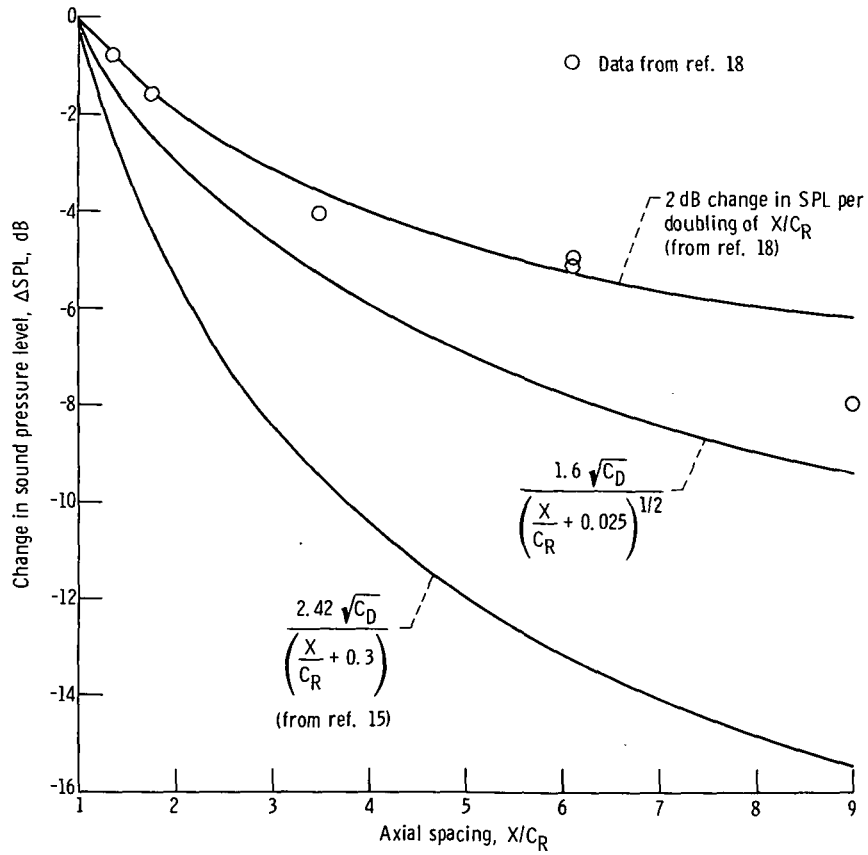


Figure 6. - Change in sound pressure level at blade passing frequency with spacing.

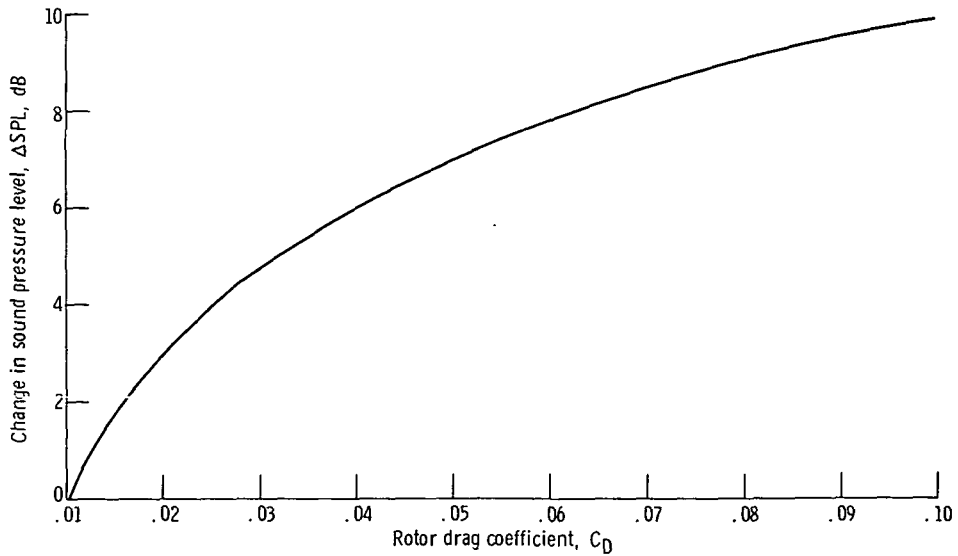


Figure 7. - Change in sound pressure level at blade passing frequency with rotor drag coefficient.

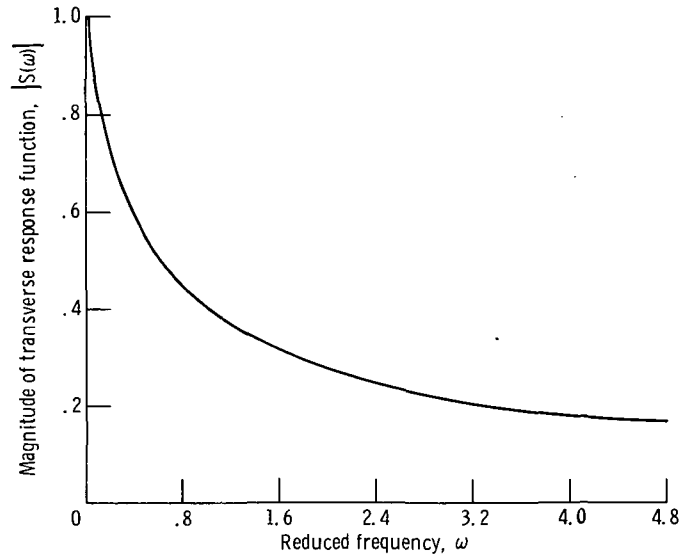


Figure 8. - Magnitude of transverse response function.

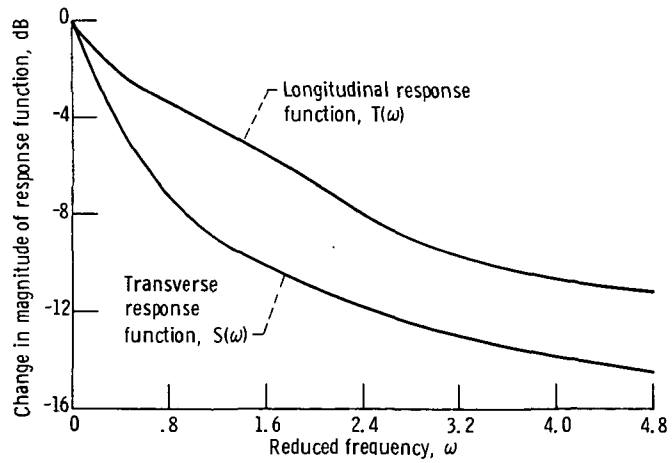


Figure 9. - Changes in magnitudes of transverse and longitudinal response functions with change in reduced frequency.



POSTMASTER: If Undeliverable (Section 1058
Postal Manual) Do Not Return

"The aeronautical and space activities of the United States shall be conducted so as to contribute to the expansion of human knowledge of phenomena in the atmosphere and space. The Administration shall provide for the widest practicable and appropriate dissemination of information concerning its activities and the results thereof."

—NATIONAL AERONAUTICS AND SPACE ACT OF 1958

NASA SCIENTIFIC AND TECHNICAL PUBLICATIONS

TECHNICAL REPORTS: Scientific and technical information considered important, complete, and a lasting contribution to existing knowledge.

TECHNICAL NOTES: Information less broad in scope but nevertheless of importance as a contribution to existing knowledge.

TECHNICAL MEMORANDUMS: Information receiving limited distribution because of preliminary data, security classification, or other reasons. Also includes conference proceedings with either limited or unlimited distribution.

CONTRACTOR REPORTS: Scientific and technical information generated under a NASA contract or grant and considered an important contribution to existing knowledge.

TECHNICAL TRANSLATIONS: Information published in a foreign language considered to merit NASA distribution in English.

SPECIAL PUBLICATIONS: Information derived from or of value to NASA activities. Publications include final reports of major projects, monographs, data compilations, handbooks, sourcebooks, and special bibliographies.

TECHNOLOGY UTILIZATION PUBLICATIONS: Information on technology used by NASA that may be of particular interest in commercial and other non-aerospace applications. Publications include Tech Briefs, Technology Utilization Reports and Technology Surveys.

Details on the availability of these publications may be obtained from:

**SCIENTIFIC AND TECHNICAL INFORMATION OFFICE
NATIONAL AERONAUTICS AND SPACE ADMINISTRATION
Washington, D.C. 20546**